

## VERTICAL ELECTRIC FIELDS AND FIELD CHANGE PARAMETERS DUE TO PARTLY INCLINED LIGHTNING LEADER CHANNELS

Chandima Gomes<sup>1, \*</sup>, Vernon Cooray<sup>2</sup>,  
and Mohd Z. A. Ab Kadir<sup>1</sup>

<sup>1</sup>Department of Electrical and Electronics Engineering, Universiti Putra Malaysia (UPM), Serdang, Selangor 43400, Malaysia

<sup>2</sup>Division for Electricity, Uppsala University, Sweden

**Abstract**—Vertical electric fields generated by lightning leader channels, the total leader field change and the total leader field change to the total return stroke field change ratio, at a certain distance, were theoretically analysed by varying the angle of orientation of a segment of upper part. Ground was treated as a perfectly conducting horizontal plane. Results were able to discern significantly large differences in the static field due to leader channels which have the same total length but a certain channel segment is oriented at different angles. The outcome of our calculations consistently explains the scatter of the total leader field observed in previous studies. Without considering such channel segment orientation, one has to assume unrealistic charge source heights or unreasonable charge densities to calculate matching values for many observed total leader fields and leader field to return stroke field ratios, labelled as anomalous observations in the literature. In some cases, irrespective of the charge source height and the charge density, one cannot find a suitable fit for the observed fields with the straight channel model.

### 1. INTRODUCTION

In this paper, we adhere to the Atmospheric science sign convention, i.e., negative polarity is assigned to the field change due to the raising of negative charge away from earth or lowering of positive charge towards earth.

---

*Received 18 August 2012, Accepted 29 October 2012, Scheduled 12 December 2012*

\* Corresponding author: Chandima Gomes (chandima.gomes@gmail.com).

Various aspects of leader fields have been studied extensively in the last few decades [1–11]. A comprehensive summary of observed leader fields available at respective time periods has been given in [8, 9].

The terminology used to describe observations is not always without ambiguity. For an example, A the definition of the beginning of the stepped leader field variation is a common confusion among scientists. The ambiguity is due to the so-called preliminary breakdown event, which occurs prior to the initiation of the leader. The duration of the preliminary variation is also not clearly defined. As discussed in [8], the initial field change that ultimately ends-up in a ground flash, is strongly related to the in-cloud discharges termed “cloud-type initial portion of the first leader field change” [12], “pre-preliminary discharge” [13], “long duration preliminary field change” [11], and “large negative pre-stroke field changes” outside the polarity reversal distance [14]. Studies such as Shao [15] have revealed that prior to stepped and dart leaders, several breakdown channels are formed in the cloud, which are not physically connected to the consequent path of the ground-directed leader.

Leader fields observed by Rakov and Uman [8] may still be the most detailed study in the subject. Their observations are based on simultaneous single station electric field and multiple station TV records of 3 convective thunderstorms occurred in Florida. They have analysed 286 strokes in 73 flashes for the leader field wave shapes. The approximate range of distance to the lightning from the measuring site has been given as 2.5–20.5 km. They classified the observed leader field wave shapes into 3 broad categories. (1) A net negative hook-shaped electric field change. (2) A net positive or zero hook-shaped electric field change. (3) A monotonic positive electric field change. They have also given examples of several cases where the leader field change is double-hook shaped or oscillatory. In the case of a number of subsequent leaders, the waveforms show a flattening (an inactive region) few milliseconds prior to the return stroke. They have given the histograms of each type of the leader fields (above categorised 3 types), with respect to distance of observation from the channel base. They have also classified the histograms by the stroke order. The first category of leader fields tends to occur at smaller distances, while the second and third categories of leader fields are observed in flashes struck further away from the place of observation. The distribution of the first category of fields tends to shift to larger distances with increasing stroke order.

Most of the research on leader fields is based on lightning measurements while in some cases a simple leader model (a line charge that extends downwards from a spherical symmetric charge or point

charge in the cloud) has been adapted to explain some observations. In many studies, where the observed leader fields are attempted to be reproduced by a simple leader model, several exceptional or anomalous cases have been found [9].

Lightning events and charge source origins are located inside the cloud by several methods. One of them is VHF mapping, in which the RF radiation emitted by cloud electric activities are observed to employ time-of-arrival or interferometric techniques, to locate the regions of activity [16–24]. The oldest, yet, widely applied method is to obtain slow field variations at several measuring stations at ground, underneath the thunder cloud to locate the charge sources [9, 11, 25, 26]. The leader field change and the ratio of the leader field change to return stroke field change, show negative values at close ranges and positive values at long distances. Thus, they have a net zero value at a particular distance. This characteristic of leader and return stroke fields (static fields) provides information to estimate the charge source heights. Taking measurements by balloon-borne instruments is also a popular method [27–30]. In some cases more than one of these techniques are applied to obtain more precise information.

Krehbiel et al. [11] have observed that three negative stepped leaders out of four that they have detected, developed horizontally in the cloud before producing a vertical extension towards ground. They have done their experiment in New Mexico, with exposed circular plate antennas at eight locations beneath the thunderstorm to obtain electrostatic field change measurements, and with the aid of 3 cm radar measurements of precipitation structure of the storm. In the single flash analysed by Rhodes and Krehbiel [20], the discharge has started with several horizontal channels developed inside the cloud, one of which culminated in the development of a negative leader to ground and a return stroke. Their observation is based on VHF/interferometric technique. This horizontal propagation of one or several discharge channels, before that or one of them diverting vertically towards ground, has clearly been observed in several other studies conducted in the same geographical location (e.g., 4 flashes in [22] and 2 flashes in [21]). Using radio interferometric technique, Hayenga and Warwick [31] have observed that the intracloud part of the lightning leaders is predominantly horizontal. Proctor [17], who recorded 26 radio images of lightning flashes, reported that many of those flashes have travelled horizontally inside the cloud before they went down vertically to ground. The observation of this inclined channel part inside the cloud is not a feature of only negative return strokes. Fuquay [32] has photographed several positive lightning channels, which have extensively long horizontal paths inside the cloud.

In some cases, these horizontal channel segments were longer than the corresponding vertical section beneath the cloud.

Kidder [33] and Carte and Kidder [34] located visible paths to ground in a number of lightning flashes, by means of a network of all-sky cameras. They have found that most of the paths below the cloud are nearly vertical. Hence, it is very convincing that a typical cloud to ground leader has a part inside the cloud that is oriented towards horizontal, followed by a nearly vertical section beneath the cloud base.

In this paper we theoretically show the dependence of the leader field (henceforth referred as  $LF$ ), the net total leader field change (henceforth referred as  $\Delta L$ ) and the total leader field change to return stroke field change ratio (henceforth referred as  $\Delta L/\Delta RS$ ) on the angle of orientation with respect to a horizontal plane (henceforth referred as  $\theta$ ) of the uppermost part of the lightning leader (henceforth referred as the oriented part), the length of which is denoted by  $h$ . In our calculations we selected the beginning of the leader proper, as the initiation of the movement of the charge from its original source location. This is the only feasible choice we have, as the observation on leader phase is somewhat ambiguous (as discussed earlier). The stepped leader and the dart leader will not be discriminated in this study. The reason is that as per several observations on in-cloud electric activity prior to ground strokes, the channel has been inclined at the upper portion in both stepped and dart leaders. As our main concern is to illustrate the dependence of  $LF$ ,  $\Delta L$  and  $\Delta L/\Delta RS$  on  $\theta$ , but not to give precise values for the two parameters, we adhered only to 2-D analysis. However, with time and effort, one can develop a computer algorithm to compute the leader and return stroke fields when the oriented part is at any direction of a 3-D hemispherical structure.

Leaders have also been observed to traverse vertically towards ground with no in-cloud horizontal part [24].  $LF$ ,  $\Delta L$  and  $\Delta L/\Delta RS$  due to leaders of such flashes fit our calculations when  $\theta$  is equal to  $90^\circ$ . Hence, the straight channel model that has been adopted in many former studies is a special case of the channel geometry that we have proposed in this paper.

Mathematically, it is convenient to assume a uniform charge distribution along the channel in calculating leader fields. However, one may expect higher charge density towards the lower tip of the leader channel as the enhancement of the capacitance of the leader, in the vicinity of the ground, drains more charge towards this region. In many leader and return stroke models the leader charge distribution is assumed either to be exponential or linear. Larson and Cooray [35] discussed the physical validity of several leader charge distributions. In

the present study, we considered a uniform charge distribution, solely due to the ease of mathematics.

Krehbiel et al. [11], in their experiment, observed that the charge distributed along the channel during the leader phase is substantially neutralised during the ensuing return stroke phase. Hence, in this study we assumed that the complete leader charge is neutralised during the return stroke phase. We also assumed that no charge is drained into the leader channel from the cloud during the return stroke phase. However, deviation of real flashes from these two assumptions may lead to the value of  $\Delta L/\Delta RS$  either greater or lower than unity for distant flashes.

Rakov and Uman [8] were the first to propose this channel geometry to calculate  $\Delta L/\Delta RS$ . They have considered a fixed length for the vertical and horizontal sections and have estimated the variation of  $\Delta L/\Delta RS$  with distance for three values of the azimuth angle,  $0^\circ$ ,  $180^\circ$  (identical to the same values of  $\theta$  in this study) and  $90^\circ$ . They were able to explain some of the observations with this model. In this study, we have given a rigorous treatment to the above subject and extended the calculations to estimate the dependence of both  $\Delta L$  and  $\Delta L/\Delta RS$  with  $\theta$  and  $h$ . We illustrate the inability of straight channel model to produce several observed values of  $\Delta L$  and  $\Delta L/\Delta RS$  that are labelled as anomalous in the literature. We also discuss the possible ambiguities that may arise when determining charge source heights and charge drained into the leader channel, with slow field measurements at ground level.

## 2. METHODOLOGY

Uman [36] constructed a simple line charge model to represent the leader channel. This has been adopted in many related studies followed. This model postulates the leader channel as a line charge that extends vertically downwards at constant speed  $v$ , from a spherically symmetric charge source centred at height  $H$ . The electric field at a distance  $D$  from the base of the channel is a result of both the charge that appear in the extending channel and the charge that disappear from the source. The electric field change due to a leader propagated for time  $t$  is given by Equation (1).

$$\Delta E = \frac{-2\rho}{4\pi\epsilon_0} \left[ \frac{1}{(D^2 + x^2)^{1/2}} - \frac{1}{(D^2 + H^2)^{1/2}} - \frac{(H - x)H}{(D^2 + H^2)^{3/2}} \right] \quad (1)$$

where  $x = H - vt$ , and  $\rho$  is the linear charge density.

The total leader field change by the time that the leader touches

the ground is obtained by making  $x = 0$  (i.e.,  $vt = H$ ).

$$\Delta L = \frac{-2\rho}{4\pi\epsilon_0} \left[ \frac{1}{D} - \frac{1}{(D^2 + H^2)^{1/2}} - \frac{H^2}{(D^2 + H^2)^{3/2}} \right] \quad (2)$$

In the return stroke phase the charge stored in the leader channel will be neutralised, thus, within the square brackets in Equation (2), only the third component is left as the total field change, after the return stroke. In other words, the total field change due to return stroke is the negative value of the first two terms of Equation (2).

The channel geometry considered for the calculation of field changes in this study is illustrated in Fig. 1. The leader field variation

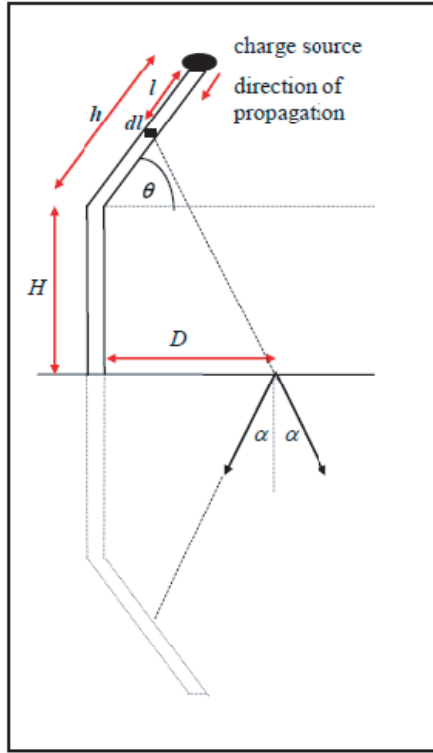


**Figure 1.** The geometry of the channel and its image that contributes to the electric field at ground at a distance  $D$  from the channel base. The arrows at distance  $D$  shows the direction of field components due to an infinitesimal channel length  $dl$  at height  $H + (h - l) \sin \theta$ . At time  $t$ ,  $l = vt$  where  $v$  is the leader speed.

at distance  $D$  at time  $t$ , due to a channel extending at speed  $v$ , is given by Equation (3).

$$\begin{aligned}
 E(t) &= \frac{-2\rho}{4\pi\epsilon_0} \int_0^{vt} \frac{(Y - v\tau \sin \theta) d(v\tau)}{\left\{ (Y - v\tau \sin \theta)^2 + (X + v\tau \cos \theta)^2 \right\}^{3/2}} \\
 &\quad - vt \frac{Y}{(Y^2 + X^2)^{3/2}} \quad \text{for } vt \leq h \\
 E(t) &= E(h/v) + \frac{-2\rho}{4\pi\epsilon_0} \left[ \frac{1}{\left\{ D^2 + (H - vt + h)^2 \right\}^{1/2}} - \frac{1}{\{D^2 + H^2\}^{1/2}} \right. \\
 &\quad \left. - (vt - h) \frac{Y}{(Y^2 + X^2)^{3/2}} \right] \quad \text{for } vt > h
 \end{aligned} \tag{3}$$

where  $X = D - h \cos \theta$  and  $Y = H + h \sin \theta$ . Note that  $l = vt$ ,  $dl = d(v\tau)$  and  $\tan \alpha = (X + vt \cos \theta)/(Y - vt \sin \theta)$  (refer Fig. 1).

The total leader field change is simply the difference between  $E[(h + H)/v]$  and  $E(0)$ . However, as we calculated  $\Delta L$  and  $\Delta L/\Delta R$  for a large number of combinations of parameters, we found that it is rather tedious and unnecessary to calculate the fields, from the time of initiation to the end, by the above equations. Thus, we obtained the above two parameters independent from calculations of  $LF$  by using Equation (4). The total leader field change is contributed by the vertical part, the oriented part and the decrement in charge at the upper end of the leader. The field contribution by the vertical part is essentially equal to the first two components (within square brackets) of Equation (2). The component of the total electric field change due to the oriented part can be obtained by integrating the contribution by each infinitesimal section of that over the whole inclined channel length. The field contribution due to the decrement in charge at the upper end is similar to the third component in Equation (2) but with modifications for the source height and the extended channel length. The total field change due to all these components is given by Equation (4).

$$\begin{aligned}
 \Delta L &= \frac{-2\rho}{4\pi\epsilon_0} \left[ \frac{1}{D} - \frac{1}{(D^2 + H^2)^{1/2}} + \int_0^h \frac{(H + l \sin \theta) dl}{\left[ (H + l \sin \theta)^2 + (D - l \cos \theta)^2 \right]^{3/2}} \right. \\
 &\quad \left. - \frac{(H + h) Y}{[Y^2 + X^2]^{3/2}} \right]
 \end{aligned} \tag{4}$$

Note that in Equation (4),  $l$  is measured from the knee point towards the charge source (i.e.,  $h - l$  in Fig. 1 has been replaced by  $l$ ).

The total return stroke field change is given by the negative sign of the first three terms within the square bracket of Equation (4). Note that as  $\theta$  goes to  $90^\circ$ , Equation (4) reduces to Equation (2) with  $H + h$  as the total channel height. When  $\theta$  is  $0^\circ$ , the oriented part directs horizontally towards the observer, and when  $\theta$  is  $180^\circ$ , it directs horizontally away from the observer.

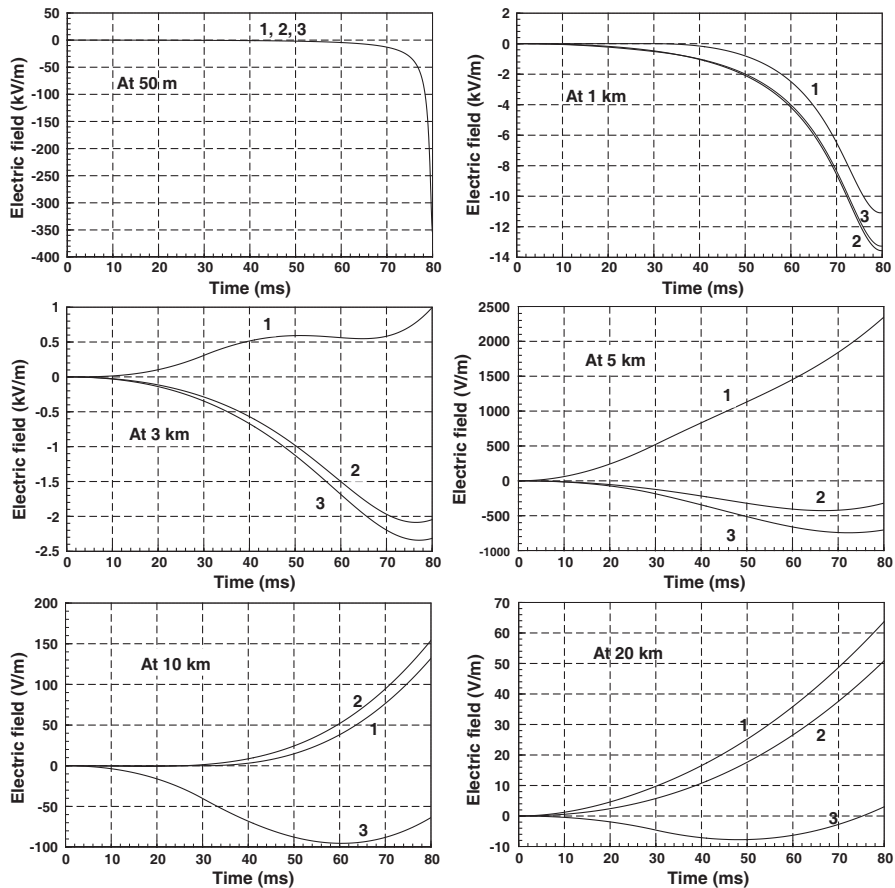
In the calculation of leader fields  $H$ ,  $h$  and  $\rho$  were given constant values of 5 km, 3 km and 0.001 C/m respectively. Angle  $\theta$  was given the values of  $0^\circ$ ,  $90^\circ$  and  $180^\circ$ . The leader speed was assumed to be  $10^5$  m/s. In the calculations of  $\Delta L$  and  $\Delta L/\Delta RS$ ,  $H$  and  $\rho$  were given fixed values of 6 km and 0.001 C/m respectively. The angle  $\theta$  was given the values  $0^\circ$ ,  $30^\circ$ ,  $45^\circ$ ,  $60^\circ$ ,  $90^\circ$ ,  $120^\circ$ ,  $135^\circ$ ,  $150^\circ$ ,  $180^\circ$  for each value of length  $h$  (which was assigned 1 km, 3 km and 6 km). For a certain  $h$  the charge drained into the leader is constant irrespective of the angle  $\theta$ . For an example when  $h$  equals 3 km the total charge funnelled into the channel is 7C. For three values of  $\theta$  (i.e.,  $0^\circ$ ,  $90^\circ$  and  $180^\circ$ ) we estimated  $\Delta L$  and  $\Delta L/\Delta RS$  by increasing  $h$  from 0 to 6 km, stepwise.

### 3. RESULTS

Figure 2 shows the leader field variation at several distances for a channel with a straight section ( $H$ ) of 5 km and an inclined part ( $h$ ) of 3 km. Curve 1, 2 and 3 correspond to  $\theta$  values of  $0^\circ$ ,  $90^\circ$  and  $180^\circ$  respectively. At very close distances (say 50 m) the channel inclination has no significance in the field variation. In the case of the upper part of the channel is oriented towards the observer, one may observe field variations with no negative excursion, even at close distance (e.g., curve 1 at 3 km). On the other hand, when the oriented part is inclined away from the observer a negative excursion can be seen in the field variation even at relatively large distances (e.g., curve 3 at 20 km). At near range (say less than 5 km) a channel with oriented part inclined away from the observer generates field variations somewhat similar to those due to straight channels. At far range (say greater than 10 km) this similarity is seen between the fields due to channels with oriented part inclined towards the observer and that due to straight channels.

Figure 3 compares the variation of leader fields, at 5 km, due to a straight channel and a channel with inclined upper part. Curve 1 corresponds to a vertical channel with height 2 km while curve 2 is pertinent to a channel with  $H$ ,  $h$  and  $\theta$  equal to 5 km, 3 km and  $0^\circ$  respectively (during the first 20 ms). Fig. 4 depicts a similar comparison, but in this case curve 1 corresponds to a leader channel

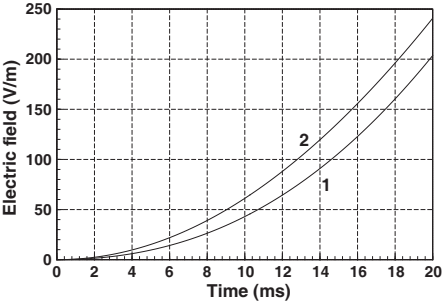




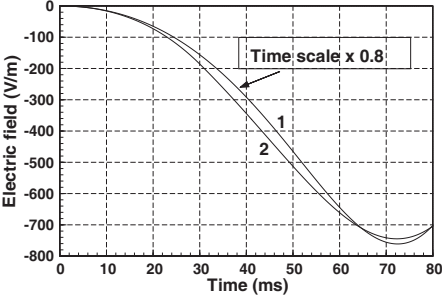
**Figure 2.** Leader fields at different distances.

with 10-km height and curve 2 is associated with a channel of  $H$ ,  $h$  and  $\theta$  equal to 5 km, 3 km and  $180^\circ$  respectively. The time scale of curve 2 is multiplied by a factor of 0.8 to view a better comparison.

The variation of  $\Delta L$  with distance from the lightning channel ( $D$ ), for several  $\theta$  values is shown in Fig. 5 where  $h$  has the values of 1 km, 3 km and 6 km respectively (in Figs. 5(a), 5(b) and 5(c)). In the three cases the total leader lengths are 7 km, 9 km and 12 km respectively. The  $\Delta L$  takes a distinct maximum value for small  $\theta$  at distance 5–10 km. For large  $\theta$ , the maximum  $\Delta L$  is oblique and it is shifted further away from the place of strike. Figs. 6(a), 6(b) and 6(c) illustrate the variation of  $\Delta L$  with  $D$ , when  $h$  is varied from zero to 6 km for  $\theta$  equals  $0^\circ$ ,  $90^\circ$  and  $180^\circ$  respectively. It is interesting to note that when



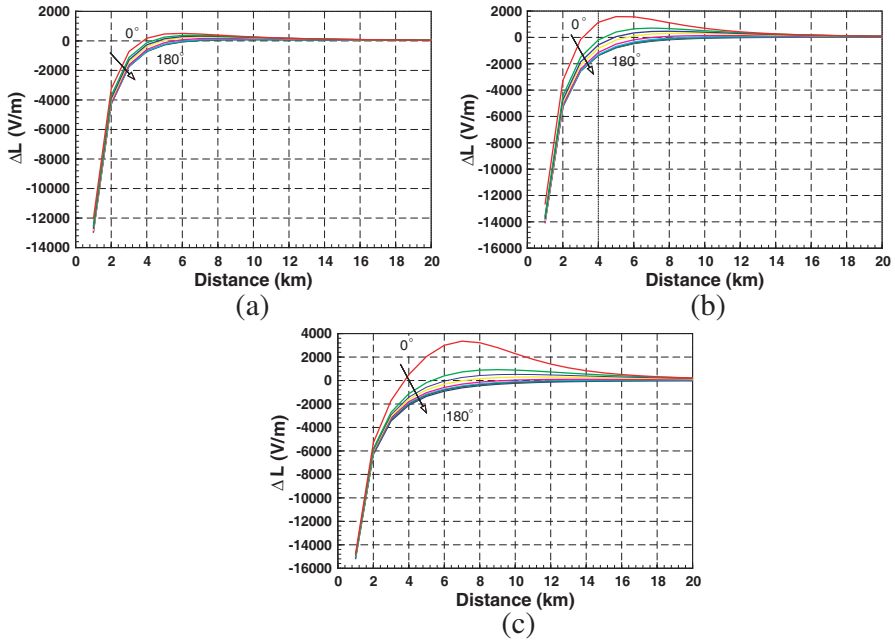
**Figure 3.** Leader field at 5 km. Curve 1 is due to a straight channel with height 2 km and Curve 2 is leader field of a channel with 5 km vertical length and 3 km horizontal upper part inclined towards the observer.



**Figure 4.** Leader field at 5 km. Curve 1 is due to a straight channel with height 10 km. The time scale of the field has been multiplied by 0.8 for the ease of comparison. Curve 2 is due to a channel with 5 km vertical length and 3 km horizontal upper part inclined away from the observer.

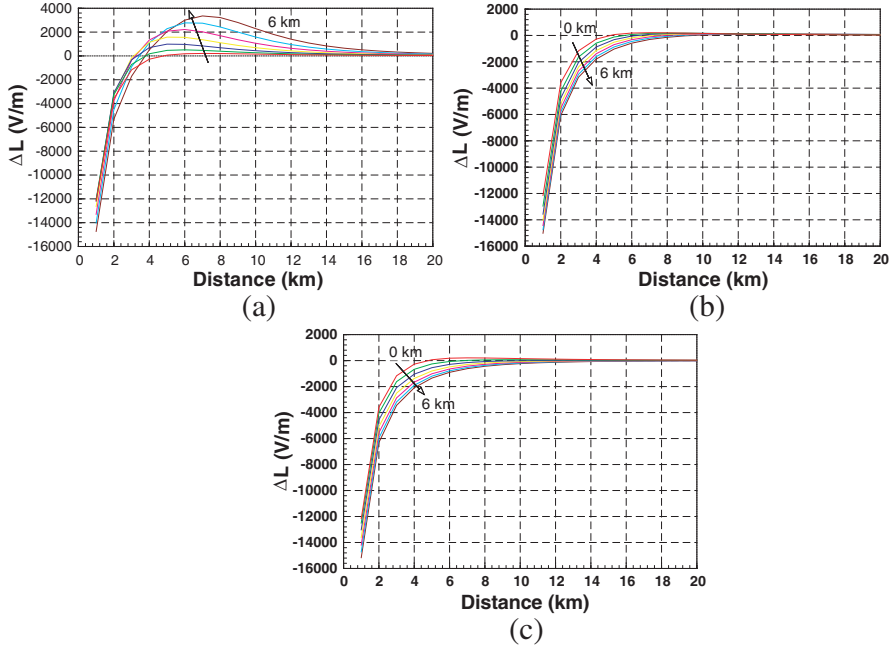
$\theta$  equals  $90^\circ$  and  $\theta$  equals  $180^\circ$ , with increasing channel height, the  $\Delta L$  curves are shifted down (i.e., at a certain distance, larger negative values for longer channel lengths) while the outcome is rather complex in the other case ( $\theta = 0^\circ$ ). In this case the curves are shifted down at distances less than about 2 km and they are shifted up at distances greater than about 6 km. In between 2 and 6 km, the variation is irregular; for an example, at distance 3 km,  $\Delta L$  becomes larger when  $h$  is increased stepwise from 1 to 3 km, and then it becomes smaller when  $h$  is increased stepwise from 3 to 6 km.

Table 1 depicts  $\Delta L$  for three values of  $\theta$  at distance 3–8 km from the lightning channel. The  $\Delta L$  for different orientations of the upper



**Figure 5.** The variation of  $\Delta L$  with  $D$ , for several  $\theta$  values. (a)  $h = 1$  km, (b)  $h = 3$  km, (c)  $h = 6$  km. The arrow indicates the direction of increasing  $\theta$ .

part of the leader channel (fixed leader length) shows large differences in value within the above range of distance. Even when the oriented part of the channel is one sixth of the vertical part of the channel (i.e.,  $h = 1$  km), there exists a considerable difference in  $\Delta L$  for different  $\theta$ . For an example, at 5 km one may observe a net total leader field change of  $-120$  V/m due to a 7-km long straight channel. One will observe a field change of  $+460$  V/m, if the topmost 1 km of the same channel is oriented horizontally towards him and  $-60$  V/m, if the same part of the channel is oriented horizontally away from him. Hence, not only the magnitude but even the polarity of  $\Delta L$  can be changed for the same channel length and at the same distance, even when a small section of the uppermost part of the leader is oriented at different angles. As one would expect, the variation of  $\Delta L$  with  $\theta$ , becomes larger with longer  $h$ . It can also be noticed that the difference in  $\Delta L$  due to a straight channel and that due to a channel with an oriented section is greatly enhanced when the oriented part is inclined towards the observer; and the difference becomes less prominent when it is inclined away from the observer. The above statement is further elaborated by



**Figure 6.** The variation of  $\Delta L$  with  $D$ , for several values (0–6 km) of  $h$ . (a)  $\theta = 0^\circ$ , (b)  $\theta = 90^\circ$ , (c)  $\theta = 180^\circ$ . The arrow indicates the direction of increasing  $h$ .

the information in Table 2 where the percentage change of  $\Delta L$  (with respect to  $\Delta L$  when  $\theta = 90^\circ$ ) for  $\theta$  equals  $0^\circ$  and  $180^\circ$  is given. The channel considered in this case has a 6 km vertical section ( $H$ ) and 3 km inclined segment ( $h$ ).

Figures 7(a), 7(b) and 7(c) illustrate the variation of  $\Delta L/\Delta RS$  with distance for different  $\theta$  values. The values of  $h$  for the curves in Figs. 7(a), (b) and (c) are 1 km, 3 km and 6 km respectively. It is obvious that for a channel where the total charge is neutralised, the  $\Delta L/\Delta RS$  reaches  $-1$  at very close distances irrespective of the channel orientation. Generally, at a certain distance the  $\Delta L/\Delta RS$  ratio decreases with increasing value of  $\theta$ . However, this general inference is violated at large distances when  $\theta$  is small and at small distances when  $\theta$  is large. Fig. 8 gives clear indication of the dependence of  $\Delta L/\Delta RS$  on  $\theta$  for a channel with  $h$  equals 3 km and the observer is at 5 km from the channel base.

Table 3 gives an indication of the variation of the distance at which  $\Delta L/\Delta RS$  becomes zero [henceforth denoted by  $(\Delta L/\Delta RS)_0$ ] with  $\theta$ .

**Table 1.**  $\Delta L$  for  $D$  from 3–8 km. The variation of the leader field change with  $\theta$  is very large at distance from 3–8 km.  $\Delta L$  is given in  $\times 10^{-2}$  V/m. (e.g., For  $h = 3$  km,  $\theta = 90^\circ$ , and  $D = 5$  km,  $\Delta L$  is  $-120$  V/m).

$h = 1$ km						
	3 km	4 km	5 km	6 km	7 km	8 km
$0^\circ$	-7.2	1.8	4.6	5.1	4.6	3.9
$90^\circ$	-16.3	-5.8	-1.2	0.8	1.5	1.8
$180^\circ$	-16.2	-6.7	-2.6	-0.7	0.2	0.5
$h = 3$ km						
	3 km	4 km	5 km	6 km	7 km	8 km
$0^\circ$	-1.6	11.4	15.8	15.6	13.6	11.1
$90^\circ$	-23.9	-11.4	-5.2	-1.8	-0.1	0.8
$180^\circ$	-25.0	-13.7	-8.0	-4.8	-3.0	-1.9
$h = 6$ km						
	3 km	4 km	5 km	6 km	7 km	8 km
$0^\circ$	-17.0	5.0	20.5	30.0	33.0	32.2
$90^\circ$	-60.1	-31.7	-18.0	-10.4	-5.8	-1.4
$180^\circ$	-34.5	-20.9	-13.5	-9.0	-6.2	-4.4

**Table 2.** For  $h = 3$  km and  $H = 6$  km the percentage change of  $\Delta L$  (with respect to a channel with  $\theta = 90^\circ$ ) for the  $\theta$  values of  $0^\circ$  and  $180^\circ$ .

$\theta$	3 km	4 km	5 km	6 km	7 km	8 km
$0^\circ$	72%	116%	214%	388%	669%	2200%
$180^\circ$	43%	34%	25%	14%	7%	214%

The  $(\Delta L/\Delta RS)_0$  is shifted away from the channel base with increasing  $\theta$  and in most of the cases with increasing  $h$ . When  $\theta$  is around  $180^\circ$  the  $(\Delta L/\Delta RS)_0$  becomes considerably larger with increasing  $h$ . However, according to Table 3, the probability of finding a  $(\Delta L/\Delta RS)_0$  greater than 10 km is considerably small.

Figures 9(a), (b) and (c) depict the  $\Delta L/\Delta RS$  for  $h$  values from 1–6 km for three values of  $\theta$  ( $0^\circ$ ,  $90^\circ$  and  $180^\circ$  respectively). The  $(\Delta L/\Delta RS)_0$  varies approximately from 3 to 4 km for  $\theta$  equals  $0^\circ$ , from 5 to 10 km for  $\theta$  equals  $90^\circ$  and from 7 km to well over 20 km for  $\theta$

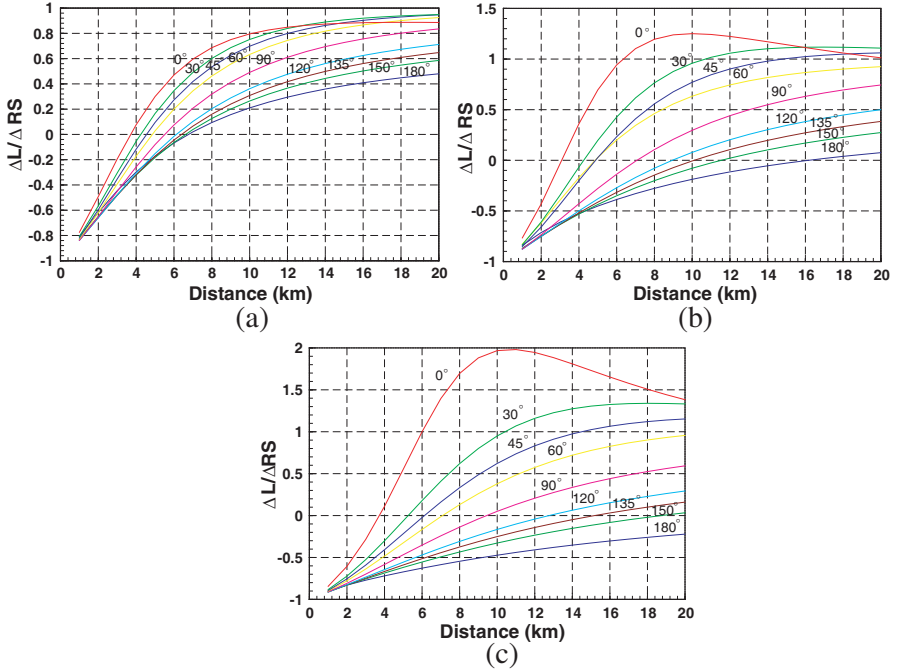


**Figure 7.** The variation of  $\Delta L/\Delta RS$  with  $D$ , for several  $\theta$  values. (a)  $h = 1$  km, (b)  $h = 3$  km, (c)  $h = 6$  km.

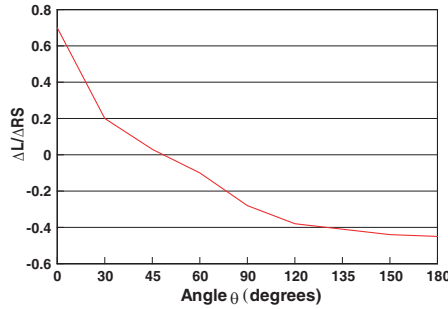


**Figure 8.** The dependence of  $\Delta L/\Delta RS$  with  $\theta$  at distance 5 km for a channel with  $h$  equals 3 km.

equals  $180^\circ$ . With this information and also with that of Table 3, it can be inferred that the  $(\Delta L/\Delta RS)_0$  is less dependent on  $h$  when the in-cloud part of the leader is oriented towards the observer and it heavily depends on  $h$  when that part of the leader is oriented away

**Table 3.**  $(\Delta L/\Delta RS)_0$  for different  $\theta$ .  $(\Delta L/\Delta RS)_0$  values are given in kilometres.

$h$ (km)	$0^\circ$	$30^\circ$	$45^\circ$	$60^\circ$	$90^\circ$	$120^\circ$	$135^\circ$	$150^\circ$	$180^\circ$
1	3.7	4.3	4.6	4.9	5.7	6.2	6.4	6.7	6.8
3	3.1	4.3	4.9	5.7	7.1	9.0	10.2	11.9	16.6
6	3.8	5.3	6.2	7.1	9.5	12.8	15.4	18.7	$> 20$

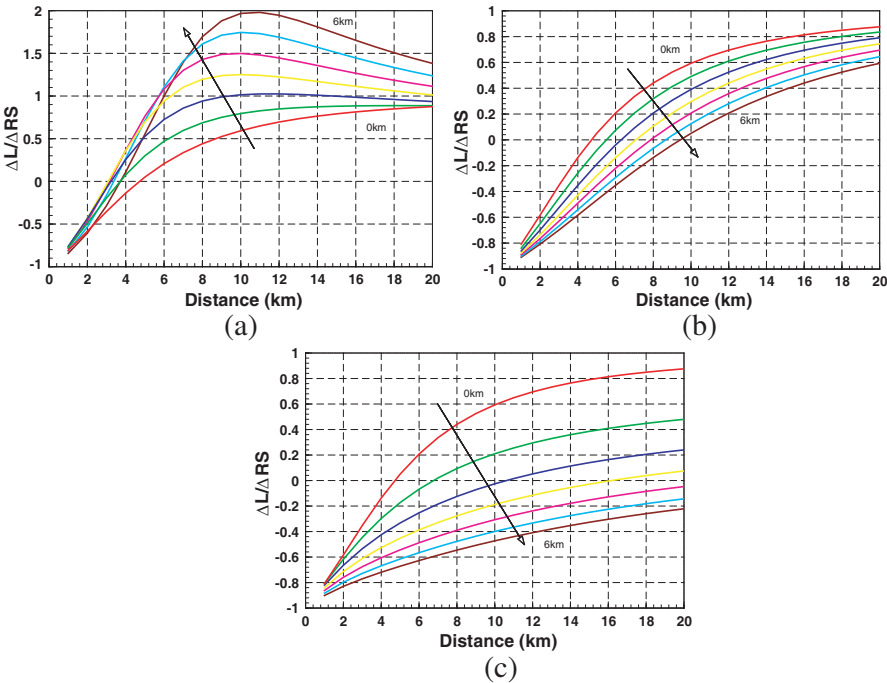


**Figure 9.** The variation of  $\Delta L/\Delta RS$  with  $D$ , for several values (0–6 km) of  $h$ . (a)  $\theta = 0^\circ$ , (b)  $\theta = 90^\circ$ , (c)  $\theta = 180^\circ$ . The arrow indicates the direction of increasing  $h$ .

from the observer. In this case too, one may see that when  $\theta$  equals  $90^\circ$  and  $180^\circ$  the  $\Delta L/\Delta RS$  curves are shifted down with increasing  $h$ . In the case where  $\theta$  equals  $0^\circ$ , these curves are shifted up at distances greater than 6 km and the variation is irregular at distances less than 6 km.

#### 4. DISCUSSION

The field variations given in Fig. 2 explain the reason for the observation of number of cases anomalous to the representative curves of leader fields at different distances as given in the literature [9, 37, 38].

It is of interest to investigate the issues raised by Beasley et al. [9] on several previous observations. One such case is the observation of leader fields with no negative excursion at close distance (3–5 km). Beasley et al. [9] explained this observation as due to a channel about 10 km away but mis-calculated by erroneous time-to-thunder measurements. This field variation is not possible to be reproduced by the straight channel model, at this distance. Although, the reasoning of [9] cannot be ruled out, this calculations show that, though it is less probable, it is not impossible to observe such fields at close distance. With a proper combination of  $H$ ,  $h$  and  $\theta$  one may reproduce  $LF$ s very similar to those observed by Appleton and Chapman [37]. The other type of fields, as described in the above publication, has an initial slow variation, followed by a steady part to the return stroke, with a short slow increase, sometimes just before the return stroke. This observation fits into the  $LF$  observed at 3 km due to a channel with  $\theta$  equals  $0^\circ$  (Fig. 2). Another unusual (in the sense that not reported in other studies) leader field change has been given in Schonland et al. [39], which they label as due to a so called  $\beta$  type leader (Fig. 4 of [39]). The field has an initial rise, which reaches a peak and gradually decreases to zero, followed by a short increase before the return stroke. Beasley et al. [9], suggested that this field variation is a result of a possible inaccuracy of the field observing technique. After several trials, we produced a similar field variation at 2.7 km for a channel with  $H$ ,  $h$  and  $\theta$  equal 5 km, 3 km and  $0^\circ$  respectively (Fig. 10). It

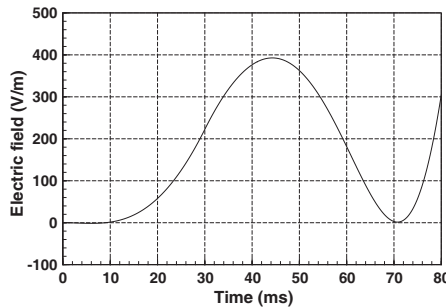


**Figure 10.** Leader field at 2.7 km. For a leader channel with  $H = 5$  km and  $h = 3$  km and  $\theta = 0^\circ$ .



might be possible to produce an even better fit for the observed field with a more suited combination of  $H$ ,  $h$ ,  $D$  and  $\theta$ . Thus, in this case too, although we do not totally discard the argument of Beasley et al. [9], It may be said that there is a certain probability, though it is slim, to observe such field variations.

This investigation shows also that the different types of leader field shapes as reported by Rakov and Uman [8] can be reproduced by channels with inclined parts. Specially, within 2–8 km, by choosing a proper combination of realistic values for  $H$ ,  $h$ , and  $\theta$ , at any given distance one can calculate a leader waveform with a negative hook-shape, a positive hook-shape, a negative/positive excursion and then flattened shape, a monotonically increasing/decreasing shape, or even a double hook-shape (e.g., one can obtain a double hook-shape when  $h$  of the leader channel in Fig. 10 is increased while keeping other parameters the same). The fact that the higher order strokes at larger distances show leader fields with negative hook-shapes, indicates that they have long horizontal parts inside the cloud.

In cases where the charge source height is determined by slow field measurements at ground, the estimation has a scatter within a broad range, for the same thunderstorm, if the sample size is large. For examples, Bernard [40]: 2.5–8.7 km amsl (above mean sea level) for 10 flashes; Jacobson and Krider [41]: 6.0–9.5 km amsl for 70 flashes; Krehbiel et al. [11]: 6.3–7.8 km amsl for 4 flashes; Krehbiel [25]: 5.2–9.3 km amsl for 26 flashes. The clear air temperature assigned to the source height, in turn, shows a large variation, which is unrealistic for the same thunderstorm. In contrast, when the same parameter is determined by VHF mapping, Radar pictures or balloon-borne measurements, this range was rather narrow. For examples, Proctor [17] radar pictures: 3.1–5.1 km above ground level for 26 flashes; Proctor [18] VHF mapping: group 1, 4.4–5.7 km amsl for 431 flashes and group 2, 7.5–9.7 km amsl for 337 flashes; Winn et al. [29] balloon-born instruments: 4.8–5.8 amsl.

The results of this study extensively account for the above contradiction in inferred information on charge source height. For one example, in the case of LF, the profile of the field due to a channel with  $H$ ,  $h$  and  $\theta$  equal 5 km, 3 km and  $0^\circ$  respectively, is similar to that of a straight channel with 2-km height (Fig. 3). Thus, one may estimate the charge source height by observing the LF due to the leader channel with the inclined part, as 2 km (assuming a straight channel model), whereas the actual height is more than twice this estimation (5 km). As it is shown in Fig. 4 when the oriented part of the same channel is inclined horizontally away from the observer ( $180^\circ$ ), the field variation matches that due to a straight channel with 10 km height. Thus, the

estimation of the charge source height, by straight channel model, will give a value two times greater.

For another example, in the observations of total field change, consider the case where  $h$  equals 1 km. A rotation of the oriented part about the knee point, by an angle of  $180^\circ$ , cause the channel length to vary between 6 and 7 km. This rotation changes  $(\Delta L/\Delta RS)_0$  from 4.7 to 6.8 km. With the straight channel model, one has to change the channel length approximately from 4 km to 11 km to account for this variation in  $(\Delta L/\Delta RS)_0$ . Note that in this example, the oriented part is only one seventh of the total channel length. The anomaly becomes even higher for larger  $h$  values.

According to the Table 1, it is clearly understood the reason why one observe both negative and positive values for the  $\Delta L$  at distance about 3–8 km (Fig. 1 of [9]), in the same thunderstorm where charge source heights do not vary distinctly from one flash to another. In the case of a straight channel, even by varying the channel height, one cannot obtain this scatter unless he assumes extremely unreasonable channel lengths (Fig. 6). The few large positive  $\Delta L$  measured around 7 km from the place of lightning strike (Fig. 1 of [9]) fit the calculated values for small  $\theta$  in our study (Fig. 5).

By the curves given in Fig. 7, we exemplify the scatter of  $\Delta L/\Delta RS$  as given in Beasley et al. [9]. By the straight channel model one has to assume unreasonably long channel lengths to explain the few small  $\Delta L/\Delta RS$  at long distances (15–20 km). With the same model, irrespective of the channel height, one cannot find suitable values to fit the large  $\Delta L/\Delta RS$  values observed at 6–10 km (Fig. 9). In this case too, the estimated  $\Delta L/\Delta RS$  curves for small  $\theta$  in our study (Fig. 7), provide consistently matching points to fit the above observation.

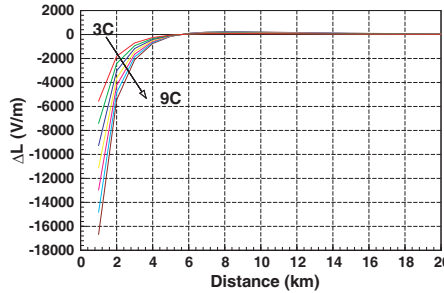


**Figure 11.** Variation of  $\Delta L$  with  $D$  for different total charge per channel values (from 3C to 9C, unit stepwise). The arrow indicates increasing charge per channel.

The dependence of  $\Delta L$  on  $\theta$  makes the determination of total charge deposited along the leader channel ambiguous. In cases where the information is inferred by single station measurements, especially at close distances, this ambiguity becomes considerably high. Fig. 11 depicts the variation in  $\Delta L$  with distance for a straight channel with length 7 km. The total charge drained into the channel has been varied from 3–9C. We compare this with Fig. 5(a) where the curves are pertinent to a channel with same length and charge (7C in the channel) but the upper one kilometre is oriented at different angles. It should be noticed that (at  $D < 4$  km) how an observer with lack of information on the channel orientation, may be lead to make erroneous conclusions on the total charge surged into the channel.

In their publication, Beasley [9] admitted that a probable explanation for the anomalous cases of  $\Delta L$  and  $\Delta L/\Delta RS$  that they have observed may be the lightning channels with horizontal parts inside the cloud. However, they have not made any attempt to estimate the influence of these channels with horizontal segments, on their results.

It is also questionable the applicability of total leader field change to return stroke field change ratio to validate return stroke models as conducted by Thottappillil et al. [42]. They have done their calculation on the consideration of a leader model with straight channel extending from a spherical symmetric charge source. All the models they have considered show  $\Delta L/\Delta RS$  values that converge to  $-1$  at close distances, which is quite consistent with experimental observations. As it was discussed earlier, irrespective of the channel orientation at very close distances  $\Delta L/\Delta RS$  reaches  $-1$ . At long distances almost all the models predict  $\Delta L/\Delta RS$  values which deviate from the experimental observations. As it was shown in our calculations the  $\Delta L/\Delta RS$  strongly varies with  $\theta$  up to 20 km, a range of distance, highly significant in the above model validating technique. Probably, the leader model that they have considered may also be accounting for this disagreement in addition to the deficiencies of the return stroke models themselves.

With this leader channel geometry, we are not able to produce the  $\Delta L/\Delta RS$  values less than  $-1$  at very close ranges, as reported in several studies [7,9]. A possible cause of this observation is the inability of the return stroke to neutralise the entire charge along the leader channel.

In this study, we have not taken into account the field variation due to a bi-directional leader, a concept which is in agreement with some observations on rocket triggered lightning and lightning strikes to air-borne vehicles [43–46]. A brief outline of this bi-directional leader

concept and the reason for the exclusion of this model in this study are given below.

Laboratory observations on a conductor in an ambient electric field, lead several researches to hypothesis and develop a bi-directional propagation model for the lightning leaders [46–48]. Once a discharge streamer is initiated at one end of the conductor an equally and oppositely charged counter streamer starts extending away from the other end of the conductor. With this observation, Kasemir [47, 48] proposed a model to represent the lightning leader channel as a prolonged spheroid, which is placed in the ambient electric field of the thundercloud. The charge at the midpoint of the spheroid is zero. The positive charge increases linearly as one progress to the upper end of the spheroid (further into the cloud). Similarly the negative charge increases linearly as one progress to the lower end of the spheroid (towards ground). The net charge on the leader is essentially zero. Once the downwards propagated leader touches the ground, a return stroke traverse the entire length of the channel, which is composed of the negative path to ground and the positive path into the cloud. The return stroke adds a uniformly distributed charge to the leader channel. Thus, in the case of a negative leader, the negative charge will be effectively neutralised at the lowermost end of the leader channel and an additional positive charge will be deposited towards the topmost end of the channel.

To suit the objectives of this study, (and also to fit into the observed channel geometry as discussed previously) any leader model that will be selected, should facilitate us to rotate a part of the leader channel inside the cloud about a knee point. In the bi-directional leader concept, the only feasible way to achieve this target is to rotate the positive part of the channel, which develops into the cloud. However, it is very complex to determine the amount and distribution of the charge that is required in the return stroke phase, in the positive part of the bi-directional leader, once it is inclined from the vertical position while the negative downward part remains vertical. Thus, within the scope of this study, we had to refrain from performing calculations for the bi-directional leader model.

It should also be emphasized that irrespective of many recent development on sophisticated field calculation models based on various computational techniques such as FDTD [49–54] we used relatively simple set of equations, yet well achieved the objectives. Hence, unless high accuracy of results is demanding for a given work purpose, it is advisable to use less-complicated models in field calculations. The same set of equations can be used in estimating leader fields in specific environments such as in marine vessels in littoral waters [55].

## 5. CONCLUSIONS

The objective of this study is to illustrate the variation of the leader field, the total leader field change and the total leader field change to the total return stroke field change ratio, at a certain distance, with the angle of inclination of a segment of the upper portion of the leader channel. We were able to discern significantly large differences in these three parameters for leader channels with the same length but a certain channel segment are oriented at different angles.

The charge source height deduced from the total leader field to return stroke field ratio seems to vary in a broad range of values even when a small segment of the leader channel changes its inclination from the vertical position. This inference accounts for the relatively wide range of source height, estimated through the slow field measurements at ground for the same thunderstorm.

The outcome of our calculations consistently explains the scatter of the total leader field and the total leader field to return stroke field ratio observed in previous studies. Otherwise, one has to assume unrealistic charge source heights or unreasonable charge densities to calculate matching values for some of the total leader fields and total leader field to return stroke field ratios, labelled as anomalous observations in the literature. In some cases, irrespective of the charge source height and the charge density, one cannot find a suitable fit with the straight channel model.

With highly developed interferometric techniques available at present for mapping electric activity inside thunderclouds, one can further evaluate the variation in  $LF$ ,  $\Delta L$  and  $\Delta L/\Delta RS$  with channel orientations that has been considered in this study. However, one may need to generalise these calculations for 3-D rotation of the oriented part of the channel prior to these results being employed in deducing related lightning parameters.

Not only the charge source height, but the total charge drained into the leader channel cannot be deduced accurately by total leader field change without taking into account the geometry of the upper part of the channel.

The results of this study force us to question the suitability of employing the total leader field change to return stroke field change ratio based on straight leader channel model, to validate return stroke models as done in the literature.

## ACKNOWLEDGMENT

The authors would like to thank the Department of Electrical and Electronics Engineering, Universiti Putra Malaysia and the Division for Electricity and Lightning Research, Uppsala University for providing excellent facilities to carry out the research. Financial support by IPPS of International Science Programs, Uppsala University, Sweden, is also acknowledged.

## REFERENCES

1. Hill, J. D., M. A. Uman, D. M. Jordan, J. R. Dwyer, and H. Rassoul, "Chaotic dart leaders in triggered lightning: Electric fields, X-rays, and source locations," *Journal of Geophysical Research*, Vol. 117, D03118, 20, 2012.
2. Shostak, V., T. Petrenko, W. Janischewskyj, and F. Rachidi, "Electric field within lightning protection volume in presence of a descending leader," *Electric Power Systems Research*, Vol. 85, 82–89, 2012.
3. Howard, J., M. A. Uman, C. Biagi, D. Hill, V. A. Rakov, and D. M. Jordan, "Measured close lightning leader step electric field-derivative waveforms," *Journal of Geophysical Research*, Vol. 116, D08201, 2011, doi:10.1029/2010JD015249.
4. Cooray, V., M. Becerra, and V. Rakov, "On the electric field at the tip of dart leaders in lightning flashes," *Journal of Atmospheric and Solar-terrestrial Physics*, Vol. 71, 1397–1404, 2009.
5. Jerauld, J., M. A. Uman, V. A. Rakov, K. J. Rambo, D. M. Jordan, and G. H. Schnetzer, "Electric and magnetic fields and field derivatives from lightning stepped leaders and first return strokes measured at distances from 100 to 1000 m," *Journal of Geophysical Research*, Vol. 113, D17111, 2008, doi:10.1029/2008JD010171.
6. Moore, C. B., K. B. Eack, G. D. Aulich, and W. Rison, "Energetic radiation associated with lightning stepped-leaders," *Geophysical Research Letters*, Vol. 28, No. 11, 2141–2144, Jun. 1, 2001.
7. Rakov, V. A., M. A. Uman, D. M. Jordan, and C. A. Priore, "Ratio of return stroke electric field change for first and subsequent lightning strokes," *Journal of Geophysical Research*, Vol. 95, 16579–16587, 1990.
8. Rakov, V. A. and M. A. Uman, "Waveforms of first and subsequent leaders in negative lightning flashes," *Journal of Geophysical Research*, Vol. 95, 16561–16577, 1990.

9. Beasley, W. H., M. A. Uman, and P. Rustan, "Electric fields preceding cloud-to-ground lightning flashes," *Journal of Geophysical Research*, Vol. 87, 4883–4902, 1982.
10. Thomson, E. M., "Characteristics of port morseby ground flashes," *Journal of Geophysical Research*, Vol. 85, 1027–1036, 1980.
11. Krehbiel, P. R., M. Brook, and R. McCroy, "An analysis of the charge structure of lightning discharges to ground," *Journal of Geophysical Research*, Vol. 84, 2432–2456, 1979.
12. Kitagawa, N. and M. Brook, "A comparison of intracloud and cloud to ground lightning discharge," *Journal of Geophysical Research*, Vol. 65, 1189–1201, 1960.
13. Ishikawa, H., "Nature of lightning discharges as origins of atmospherics," *Proceedings of the Research Institute of Atmospherics*, Vol. 8A, 1–273, Nagoya University, 1961.
14. Thomson, E. M., "Characteristics of port morseby ground flashes," *Journal of Geophysical Research*, Vol. 85, 1027–1036, 1980.
15. Shao, X. M., "The development and structure of lightning discharges observed by VHF radio interferometry," Ph.D. Thesis, University of Florida, USA, 1993.
16. Proctor, D. E., "VHF radio pictures of cloud flashes," *Journal of Geophysical Research*, Vol. 86, 4041–4071, 1981.
17. Proctor, D. E., "Lightning and precipitation in a small multicellular thunder storm," *Journal of Geophysical Research*, Vol. 88, 5421–5440, 1983.
18. Proctor, D. E., "Regions where lightning flashes began," *Journal of Geophysical Research*, Vol. 96, 5099–5112, 1991.
19. Proctor, D. E., R. Uytenbogaardt, and B. M. Meridith, "VHF radio pictures of lightning flashes to ground," *Journal of Geophysical Research*, Vol. 93, 12683–12727, 1988.
20. Rhodes, C. T. and P. R. Krehbiel, "Interferometric observations of a single cloud-to-ground flash," *Geophysical Research Letters*, Vol. 16, 1169–1172, 1989.
21. Rhodes, C. T., X. M. Shao, P. R. Krehbiel, R. J. Thomas, and C. O. Hayenga, "Observations of lightning phenomena using radio interferometry," *Journal of Geophysical Research*, Vol. 99, 13059–13082, 1994.
22. Shao, X. M., "The development and structure of lightning discharges observed by VHF radio interferometry," Ph.D. Thesis, University of Florida, USA, 1993.

23. Shao, X. M. and P. R. Krehbiel, "The spatial and temporal development of intracloud lightning," *Journal of Geophysical Research*, Vol. 101, No. 26, 26641–26668, 1996.
24. Rustan, P. L., M. A. Uman, D. G. Childers, W. H. Beasley, and C. L. Lennon, "Lightning source location from VHF radiation data for a flash at the Kennedy Space Centre," *Journal of Geophysical Research*, Vol. 85, 4893–4903, 1980.
25. Krehbiel, P. R., "An analysis of the electric field change produced by lightning," Ph.D. Thesis, University of Manchester Institute of Science and Technology, UK, 1981.
26. Maier, L. M. and E. P. Krider, "The charges that are deposited by cloud-to-ground lightning in Florida," *Journal of Geophysical Research*, Vol. 91, 13275–13289, 1986.
27. Marshall, T. C., W. Rison, W. D. Rust, M. Stolzunberg, J. C. Willett, and W. P. Winn, "Rocket and balloon observations of electric fields in two thunderstorms," *Journal of Geophysical Research*, Vol. 100, No. 20, 20815–20828, 1995.
28. Marshall, T. C. and W. D. Rust, "Two types of vertical electric structures in stratiform precipitation regions of mesoscale convective systems," *Bulletin of the American Meteorological Society*, Vol. 74, 2159–2170, 1993.
29. Winn, W. P., C. B. Moore, and C. R. Holmes, "Electric field structure in active part of a small, isolated thundercloud," *Journal of Geophysical Research*, Vol. 86, 1187–1193, 1981.
30. Byrne, G. J., A. A. Few, and M. E. Weber, "Altitude, thickness and charge concentration of charged regions of four thunderstorms during TRIP 1981 based upon in situ balloon electric field measurements," *Geophysical Research Letters*, Vol. 10, 39–42, 1983.
31. Hayenga, C. O. and J. W. Warwick, "Two-dimensional interferometric positions of VHF lightning sources," *Journal of Geophysical Research*, Vol. 86, 7451–7462, 1981.
32. Fuquay, D. M., "Positive cloud to ground lightning in summer thunderstorms," *Journal of Geophysical Research*, Vol. 87, 7131–7140, 1982.
33. Kidder, R. E., "The location of lightning flashes at ranges less than 100 km," *Journal of Atmospheric and Terrestrial Physics*, Vol. 35, 283–290, 1973.
34. Carte, A. E. and R. E. Kidder, "Lightning in relation to precipitation," *Journal of Atmospheric and Terrestrial Physics*, Vol. 39, 139–148, 1977.



35. Larsson, A. and V. Cooray, "Charge distribution in the lightning leader channel," *Proc. 23rd Int. Conf. on Lightning Protection*, 56–60, Florence, Italy, 1996.
36. Uman, M. A., *Lightning*, 48–59, Dover Publication, NY, 1969.
37. Appleton, E. V. and F. W. Chapman, "On the nature of Atmospherics, IV," *Proceedings of the Royal Society of London, Series A*, Vol. 158, 1–22, 1937.
38. Clarence, N. D. and D. J. Malan, "Preliminary discharge processes in lightning flashes to ground," *Q. J. Roy. Meteorol. Soc.*, Vol. 83, 161–172, 1957.
39. Schonland, B. F. J., D. B. Hodges, and H. Collens, "Progressive lightning-5, A comparison of photographic and electrical studies of the discharge process," *Proceedings of the Royal Society of London, Series A*, Vol. 166, 56–75, 1938.
40. Barnard, V., "The approximate mean height of the thundercloud charges taking part in a flash to ground," *Journal of Geophysical Research*, Vol. 56, 33–35, 1951.
41. Jacobson, E. A. and E. P. Krider, "Electrostatic field changes produced by Florida lightning," *J. Atmos. Sci.*, Vol. 33, 103–117, 1976.
42. Thottappillil, R., V. A. Rakov, and M. A. Uman, "Distribution of charge along the lightning channel: Relation to remote electric and magnetic fields and return stroke models," *Journal of Geophysical Research*, Vol. 102, 6987–7006, 1997.
43. Laroche, P., V. Idone, A. Eybert-Berard, and L. Barret, "Observations of bi-directional leader development in triggered lightning flash," *International Aerospace and Grounding Conference on Lightning and Static Electricity*, Cocoa Beach, Florida, USA, 1991.
44. Mazur, V., "Triggered lightning strikes to aircraft and natural intracloud discharges," *Journal of Geophysical Research*, Vol. 94, 3311–3325, 1989.
45. Mazur, V., "Physical model of lightning initiation on aircraft in thunderstorms," *Journal of Geophysical Research*, Vol. 94, 3326–3340, 1989.
46. Mazur, V. and L. H. Runhke, "Common physical processes in natural and artificially triggered lightning," *Journal of Geophysical Research*, Vol. 98, 12913–12930, 1993.
47. Kasemir, H. W., "A contribution to the electrostatic theory of a lightning discharge," *Journal of Geophysical Research*, Vol. 65, 1873–1878, 1960.

48. Kasemir, H. W., "Static discharge and triggered lightning, international aerospace and grounding conference on lightning and static electricity," DOT/FAA/CT-83/25, 24.1–24.11, 1983.
49. Izadi, M., M. Z. A. Ab Kadir, C. Gomes, V. Cooray, and J. Shoene, "Evaluation of lightning current and velocity profiles along lightning channel using measured magnetic flux density," *Progress In Electromagnetic Research*, Vol. 130, 473–492, 2012.
50. Izadi, M., M. Z. A. Ab Kadir, C. Gomes, and V. Cooray, "Evaluation of lightning return stroke current using measured electromagnetic fields," *Progress In Electromagnetic Research*, Vol. 130, 581–600, 2012.
51. Izadi, M., M. Z. A. Ab Kadir, C. Gomes, and V. Cooray, "Evaluation of lightning return stroke parameters using measured magnetic flux density and PSO algorithm," *Electrical Review Journal-Przegląd Elektrotechniczny*, Vol. 88, NR 10A/2012, 201–204, 2012.
52. Javor, V., "Modeling of lightning strokes using two-peaked channel-base currents," *International Journal of Antennas and Propagation*, Art No. 318417, 2012.
53. Izadi, M., M. Z. Ab. Kadir, C. Gomes, and W. F. Wan Ahmad, "Numerical expressions in time domain for electromagnetic fields due to lightning channels," *International Journal of Applied Electromagnetics and Mechanics*, Vol. 37, 1–15, 2011.
54. Izadi, M., M. Z. A. A. Kadir, and C. Gomes, "Evaluation of electromagnetic fields associated with inclined lightning channel using second order FDTD-hybrid methods," *Progress In Electromagnetic Research*, Vol. 117, 209–236, 2011.
55. Gomes, C. and M. Z. A. Ab. Kadir, "Protection of naval systems against electromagnetic effects due to lightning," *Progress In Electromagnetic Research*, Vol. 113, 333–349, 2011.